Original Article

MOLECULAR METABOLISM

Interaction between magnesium and methylglyoxal in diabetic polyneuropathy and neuronal models

Alexander Strom [1,2,], Klaus Strassburger [2,3], Martin Schmuck [4], Hanna Shevalye [5], Eric Davidson [5], Fariba Zivehe [1], Gidon Bönhof [1], Rudolph Reimer [6], Bengt-Frederik Belgardt [2,7], Thomas Fleming [8], Barbara Biermann [9], Volker Burkart [1,2], Karsten Müssig [1,2,10], Julia Szendroedi [1,2,10], Mark A. Yorek [5,11], Ellen Fritsche [4], Peter P. Nawroth [2,8], Michael Roden [1,2,10], Dan Ziegler [1,2,10,*], for the GDS Group**

ABSTRACT

Objective: The lack of effective treatments against diabetic sensorimotor polyneuropathy demands the search for new strategies to combat or prevent the condition. Because reduced magnesium and increased methylglyoxal levels have been implicated in the development of both type 2 diabetes and neuropathic pain, we aimed to assess the putative interplay of both molecules with diabetic sensorimotor polyneuropathy.

Methods: In a cross-sectional study, serum magnesium and plasma methylglyoxal levels were measured in recently diagnosed type 2 diabetes patients with (n = 51) and without (n = 184) diabetic sensorimotor polyneuropathy from the German Diabetes Study baseline cohort. Peripheral nerve function was assessed using nerve conduction velocity and quantitative sensory testing. Human neuroblastoma cells (SH-SY5Y) and mouse dorsal root ganglia cells were used to characterize the neurotoxic effect of methylglyoxal and/or neuroprotective effect of magnesium.

Results: Here, we demonstrate that serum magnesium concentration was reduced in recently diagnosed type 2 diabetes patients with diabetic sensorimotor polyneuropathy and inversely associated with plasma methylglyoxal concentration. Magnesium, methylglyoxal, and, importantly, their interaction were strongly interrelated with methylglyoxal-dependent nerve dysfunction and were predictive of changes in nerve function. Magnesium supplementation prevented methylglyoxal neurotoxicity in differentiated SH-SY5Y neuron-like cells due to reduction of intracellular methylglyoxal formation, while supplementation with the divalent cations zinc and manganese had no effect on methylglyoxal neurotoxicity. Furthermore, the downregulation of mitochondrial activity in mouse dorsal root ganglia cells and consequently the enrichment of triosephosphates, the primary source of methylglyoxal, resulted in neurite degeneration, which was completely prevented through magnesium supplementation.

Conclusions: These multifaceted findings reveal a novel putative pathophysiological pathway of hypomagnesemia-induced carbonyl stress leading to neuronal damage and merit further investigations not only for diabetic sensorimotor polyneuropathy but also other neurodegenerative diseases associated with magnesium deficiency and impaired energy metabolism.

Keywords Recent-onset type 2 diabetes; Diabetic sensorimotor polyneuropathy; Carbonyl stress; Methylglyoxal; Hypomagnesemia

1. INTRODUCTION

Diabetic sensorimotor polyneuropathy (DSPN) accounts for ~75% of diabetic neuropathies and is encountered in approximately 30% of people with diabetes [1]. While reliable diagnostic methods for DSPN are available, the underlying mechanisms of this condition remain incompletely understood, and therapies for treatment or prevention are lacking.

[1]Institute for Clinical Diabetology, German Diabetes Center at Heinrich Heine University, Leibniz Center for Diabetes Research, Düsseldorf, Germany [2]German Center for Diabetes Research (DZD), München-Neuherberg, Germany [3]Institute for Biometrics and Epidemiology, German Diabetes Center at Heinrich Heine University, Leibniz Center for Diabetes Research, Düsseldorf, Germany [4]IUF - Leibniz Research Institute for Environmental Medicine, Düsseldorf, Germany [5]Department of Internal Medicine, University of Iowa, Iowa City, USA [6]Microscopy and Image Analysis Technology Platform, Heinrich Pette Institute, Leibniz Institute for Experimental Virology, Hamburg, Germany [7]Institute for Vascular and Islet Cell Biology, German Diabetes Center at Heinrich Heine University, Leibniz Center for Diabetes Research, Düsseldorf, Germany [8]Department of Medicine I and Clinical Chemistry, University Hospital Heidelberg, Heidelberg, Germany [9]Institute of Neural and Sensory Physiology, Medical Faculty, University of Düsseldorf, Düsseldorf, Germany [10]Division of Endocrinology and Diabetology, Medical Faculty, Heinrich Heine University, Düsseldorf, Germany [11]Iowa City VA Healthcare System, Iowa City, USA

*Corresponding author. German Diabetes Center, Auf'm Hennekamp 65, 40225 Düsseldorf, Germany. E-mail: dan.ziegler@ddz.de (D. Ziegler).

**Corresponding author. German Diabetes Center, Auf'm Hennekamp 65, 40225 Düsseldorf, Germany. E-mail: alexander.strom@ddz.de (A. Strom).

Abbreviations: AGEs, Advanced glycation end-products; BSA, bovine serum albumin; DRG, dorsal root ganglia; DSPN, diabetic sensorimotor polyneuropathy; GDS, German Diabetes Study; GLO1, glyoxalase 1; GLO2, Glyoxalase 2; PDH, pyruvate dehydrogenase; PFA, paraformaldehyde; TDT, thermal detection threshold

Received September 28, 2020 • Revision received November 4, 2020 • Accepted November 5, 2020 • Available online 6 November 2020

https://doi.org/10.1016/j.molmet.2020.101114

Methylglyoxal is highly reactive and one of the most potent dicarbonyls leading to the formation of advanced glycation end-products (AGEs), non-enzymatic protein and DNA modifications formed under influence of glycemic and oxidative stress. Methylglyoxal originates mainly from glucose and fructose metabolism or enzymatic and non-enzymatic reactions of lipid and amino acid metabolism [2]. The enzymes glyoxalase 1 (GLO I) and glyoxalase 2 (GLO2) form the integral parts of the glyoxalase pathway. Methylglyoxal toxicity is closely associated with GLO1 activity, which is the rate limiting step in the methylglyoxal degradation [3].

Systemic methylglyoxal concentrations are increased in patients with diabetes [4,5]. It has recently been suggested that increased methylglyoxal levels recapitulate several aspects of type 2 diabetes, such as obesity, hyperglycemia, and insulin resistance [6]. In hyperglycemia, the higher glucose flux results in an accumulation of triosephosphates [7], which in turn leads to increased formation of methylglyoxal [5,8]. Neuronal tissue has a high demand for energy, the exclusive source of which is glucose, absorbed in large amounts independent of insulin under normoglycemic conditions. Thus, in diabetes, neuronal tissue is exposed to a higher risk of methylglyoxal formation and accumulation. We previously reported that methylglyoxal depolarizes sensory neurons and induces post-translational modifications of the voltage-gated sodium channel Nav1.8 [9]. Furthermore, several experimental and clinical studies have demonstrated increased glycation of neuronal tissue in diabetes [10–12], and various approaches to preventing AGE formation or binding of AGEs to receptors improved experimental diabetic neuropathy [13–15]. However, clinical studies assessing the role of methylglyoxal in patients with diabetic neuropathy have shown contradictory results [16–18], while the putative mechanisms of methylglyoxal-induced DSPN remain unknown.

Magnesium is the second most abundant intracellular divalent cation. It is involved in several hundreds of metabolic reactions where it mainly serves as a cofactor [19]. Magnesium plays an important role in carbohydrate metabolism and cellular bioenergetics. For example, magnesium is a crucial cofactor for carbohydrate metabolism enzymes, including pyruvate dehydrogenase (PDH) [20], α-ketoglutarate dehydrogenase [21], and transketolase [22]. There is substantial evidence from epidemiological studies suggesting that both decreased magnesium intake and magnesium status are associated with prediabetes and diabetes [23,24]. Furthermore, a recent cross-sectional study demonstrated that low serum magnesium levels are associated with DSPN in patients with type 2 diabetes [25]. Another study showed that lower serum magnesium levels are associated with a lower composite z score of compound muscle action potential and sensory nerve action potential amplitudes in type 2 diabetes patients recruited from a Chinese tertiary diabetes center, indicating that low serum magnesium levels could affect peripheral nerve function through axonal degeneration [26]. In experimental studies, oral magnesium administration prevented diabetes induced thermal hyperalgesia in rats [27] and improved nerve function and fostered nerve regeneration in mice with a sciatic nerve injury [28].

Enhanced glycation processes have been suggested to play a role in the development and progression of long-term diabetic complications, including DSPN. In addition to its neuroprotective effect [29], magnesium plays an important role in glucose metabolism [23,30]. Here, we reveal a putative link of methylglyoxal and magnesium with DSPN in recently diagnosed type 2 diabetes patients.

2. MATERIALS AND METHODS

2.1. Volunteers

The study was approved by the local ethics committee (Heinrich Heine University, Düsseldorf). All participants provided written informed consent according to the Declaration of Helsinki. Volunteers were participants of the prospective German Diabetes Study (GDS) and were recruited consecutively at the German Diabetes Center in Düsseldorf. GDS evaluates the long-term course of diabetes and its sequelae (ClinicalTrials.gov Identifier: NCT01055093). A detailed study design and cohort profile were described previously [31].

2.2. Peripheral nerve function

Nerve conduction velocity and quantitative sensory testing (QST) were performed as previously described [32]. Median, ulnar, and peroneal motor nerve conduction velocity (MNCV) as well as median, ulnar, and sural sensory nerve conduction velocity (SNCV) were measured at a skin temperature of 33–34 °C using surface electrodes (Nicolet VikingQuest, Natus Medical, San Carlos, CA, USA). QST included assessment of vibration perception threshold (VPT) at the second metacarpal bone and medial malleolus using the method of limits (Vibrameter, Somedic, Stockholm, Sweden) and thermal detection thresholds (TDT) following warm and cold stimuli at the thenar eminence and dorsum of the foot using the method of limits (TSA-II NeuroSensory Analyzer, Medoc, Ramat Yishai, Israel). Neurological examination was performed using the Neuropathy Disability Score (NDS) and Neuropathy Symptom Score (NSS) [33]. DSPN was defined according to modified Toronto Consensus criteria [34]: *Subclinical DSPN (Stage 1a)*: NDS$\leq$2 points, NSS$\leq$2 points, and nerve conduction studies (NCS) $<$ 2.5th percentile; *confirmed asymptomatic DSPN (Stage 1b)*: NDS $\geq$3 points, NSS $\leq$2 points, and NCS$<$2.5th percentile; *confirmed symptomatic DSPN (Stage 2)*: NSS $\geq$3 points and NCS$<$2.5th percentile.

2.3. Measurement of serum magnesium concentrations

Serum magnesium levels were determined in the baseline cohort of the GDS participants and in the subgroup of individuals with a 5-year follow-up using a Cobas c311 clinical chemistry analyzer (Roche Diagnostic, Germany).

2.4. Measurement of plasma methylglyoxal concentrations

Plasma methylglyoxal was determined at the Department of Medicine I and Clinical Chemistry (University Hospital Heidelberg) in the GDS baseline cohort using high-performance liquid chromatography (HPLC) after derivatization with 1,2-diamino-4,5-dimethoxybenezene as previously described [5]. To prevent overestimation of methylglyoxal levels by peroxidases and trace metals, derivatization was performed in the presence of sodium azide and diethylenetriaminepentaacetic acid (DETAPAC), as described [35].

2.5. Compounds

Methylglyoxal solution (M0252; Sigma Aldrich, Germany). Retinoic acid (R2625; Sigma Aldrich) - transcriptional factor of cell growth and differentiation. 6,8-Bis(benzylthio)-octanoic acid (CPI-613) (SML0404; Sigma Aldrich, Germany) - E1α pyruvate dehydrogenase modulator.

2.6. SH-SY5Y cell culture and differentiation

The human neuroblastoma SH-SY5Y cell line, obtained from Deutsche Sammlung von Mikroorganismen und Zellkulturen (DSMZ, Germany), was maintained at 37 °C in a humidified atmosphere of 5% CO_2. Cells were propagated in high glucose (25 mM) Dulbecco's Modified Eagle

Medium (DMEM) GlutaMax supplemented with 10% fetal bovine serum (FBS), 25 mM HEPES, 1 mM pyruvate, 1,000 U/mL penicillin, 1,000 μg/mL streptomycin, and non-essential amino acids.
For neuronal differentiation, 1 mL/slide of cell suspension ($1-4 \times 10^5$ cells) was transferred on sterile microscopy slides (Flex slides (DAKO), Agilent Technologies, Germany), placed within a petri dish, and incubated for 24 h. The medium was then removed, and 10 mL/dish of medium supplemented with 10 μM of retinoic acid (Sigma Aldrich, Germany) was added. During the differentiation process of 7 days, retinoic acid supplemented medium was renewed every 2–3 days.

2.7. Treatment of differentiated cells

It has been shown previously that exposure of undifferentiated SH-SY5Y neuroblastoma cells to 500 μM methylglyoxal results in a reduction of cell viability by 50% [36]. Therefore, differentiated SH-SY5Y cells were treated with 0, 400, and 800 μM of methylglyoxal either alone or with 30 mM of $MgCl_2$ (Sigma Aldrich, Germany) for 24 h.

2.8. Immunocytochemical staining

Following the treatments, SH-SY5Y cells and primary cortical neurons were fixed in 4% paraformaldehyde (PFA) for 30 min at 37 °C by adding 1 mL of 20% PFA solution (Electron Microscopy Sciences, Hatfield, PA, USA) per 4 mL of medium. After fixation, cells were washed 3 times with phosphate-buffered saline (PBS) and incubated for 1 h at room temperature with primary antibodies diluted in 5% Protein Block solution (DAKO, Denmark) containing 0.1% Triton-X: rabbit anti-β-tubulin III (1:200; Sigma Aldrich, Germany) or rabbit anti-α-tubulin (1:1,000; Abcam, Germany) and mouse anti-MG-H1 (1H7G5) (1:250; Hycultec GmbH, Germany). Cells were then washed 3 times with PBS and incubated with 1:600 donkey anti-rabbit-Alexa488 and donkey anti-mouse-Alexa568 secondary antibodies (Thermo Fisher Scientific, Germany) and 1 mg/mL Hoechst (Sigma Aldrich, Germany) for 30 min at room temperature.

2.9. High-content image analysis (HCA) of SH-SY5Y cells

The Cellomics ArrayScan VTI platform (Thermo Fisher Scientific, Germany) was used to acquire images (60 images/channel). In brief, 512 × 512 pixel (1 pixel = 0.645 μm) 16-bit images were acquired using an LD Plan Neofluar 20 × /0.4 objective (Zeiss, Germany) with a 4′,6-diamidino-2-phenylindole (DAPI) filter for nuclear staining and a BGRFR-386-23 filter for neuronal staining. Neuronal count and neuronal morphology were analyzed with the Neuronal Profiling Bioapplication software v4.1 (*NPBA*, Thermo Fisher Scientific).

2.10. Analyses of protein expression and modification

Treated SH-SY5Y cells were lysed using RIPA lysis buffer (Sigma Aldrich, Germany) containing complete protease inhibitor and PhosStop phosphatase inhibitor cocktail for 2 h at 4 °C on a rotation-shaker. The lysate was centrifuged at 10,000×*g* for 15 min and the supernatant stored at −20 °C. For western blot analyses, protein samples of the corresponding lysates were separated by sodium dodecyl sulfate polyacrylamide gel electrophoresis (SDS-PAGE) using 10% horizontal gels and transferred onto Immobilon-P transfer membranes (Merck Millipore, Germany) in a semi-dry blotting apparatus. The membranes were blocked for 1 h with tris-buffered saline (TBS) containing 0.1% Tween and 5% non-fat dry milk at room temperature. Subsequently, the membranes were incubated overnight with corresponding primary antibodies mouse anti-MG-H1 (1H7G5) (Hycultec GmbH, Germany) or rabbit anti-β-actin (Abcam). After washing 3 times with TBS-Tween, the membranes were incubated with corresponding secondary horseradish peroxidase (HRP)-coupled antibody (Promega, Germany). Enhanced chemiluminescence detection using Immobilon HRP substrate (Millipore, USA) was used to process the membrane. Signals were visualized using the Chemidoc station and analyzed with the Image Lab 5.2 software (BioRad, Germany). To minimize the possibility of unequal total protein load, the level of MG-H1 protein modifications was normalized to β-actin level in the corresponding sample.

2.11. Adult mouse sensory neuron culture

The experiments were performed at the Department of Internal Medicine (University of Iowa) in accordance with regulations specified by the National Institutes of Health "Principles of Laboratory Animal Care" and Iowa City VA Health Care System (IACUC approval number: 1891201). Adult mouse sensory neurons were isolated from dorsal root ganglia (DRG) and grown in culture as described in [37]. Twelve-week-old C57Bl/6J mice were anesthetized with Nembutal (75 mg/kg, i.p., Abbott Laboratories, North Chicago, IL) and euthanized by cervical dislocation. All cervical through lumbar level DRG were dissected aseptically from vertebral column and placed in ice-cold Ca^{2+}/Mg^{2+} free Hanks' balanced salt solution ([HBSS], Gibco, Life Technologies Corporation, Grand Island, NY, USA). Care was taken to remove spinal nerves connected to the ganglia. Enzymatic dissociation was performed by incubating DRG with 40 U/mL papain and 0.7 mg/ml L-Cystein in Ca^{2+}/Mg^{2+} free HBSS for 20 min at 37 °C, followed by incubation with 4 mg/mL of collagenase A (Roche Diagnostics, Mannheim, Germany) and 2 mg/mL of dispase (Gibco, Life Technologies Corporation, Grand Island, NY, USA) in Ca^{2+}/Mg^{2+} free HBSS for 20 min at 37 °C. The enzyme solutions were kept in cell culture incubator at 37 °C and 5% CO2 for 30 min prior to their addition to ganglia. DRG were triturated in L-15 medium (Gibco, Life Technologies Corporation, Grand Island, NY, USA) and neurons were separated from debris and Schwann cells by centrifugation through a column of 15% fatty acid free bovine serum albumin ([BSA], Roche Diagnostics, Mannheim, Germany) in L-15 as described in [38]. After washing, cells were gently resuspended in complete F-12 medium (Gibco, Life Technologies Corporation, Grand Island, NY, USA) supplemented with 1% fatty acid free BSA, 100 U/mL penicillin, 100 μg/mL streptomycin, and N-2 supplement. No exogenous growth factors were added at this point. Neurons were plated on poly-D-lysine/laminin Biocoat glass coverslips (Corning, Discovery Labware, Inc., Bedford, MA, USA) and were allowed to adhere for 2 h at 37 °C and 5% CO2. Coverslips were then flooded with pre-warmed complete F-12 medium with 50 ng/mL nerve growth factor (NGF), or 5, 10, or 15 nM magnesium chloride or combination of 1 nM of antimycin A and 16 μM of CPI-613 (6,8-Bis(bezylthio)-octanoic acid) with or without 5, 10, or 15 mM of magnesium chloride and incubated for 24 h. For the control condition, cells were incubated in complete F-12 medium without nerve growth factor.

2.12. Fluorescence immunocytochemistry and quantification of neurite outgrowth in the DRG culture

After 24 h, the coverslips were washed twice with Ca++/Mg++ free 100 mM of PBS, pH 7.4 and fixed with 4% formaldehyde (Polysciences, Inc., Warrington, PA, USA) in 100 mM of PBS for 20 min. Non-specific binding was blocked by 1% BSA, 1% normal goat serum, and 0.1% Triton X-100 in 20 mM of PBS at room temperature for 30 min. The blocking step was followed by incubation with neuronal class III β-tubulin mouse monoclonal antibody (clone TUJ1,1:1,000 working dilution, Biolegend, San Diego, CA, USA) overnight at 4 °C and then with secondary Alexa Fluor 546 conjugated goat anti-mouse

antibody (1:2,000 working dilution, Invitrogen, Life Technologies Corporation, Eugene, OR, USA) for 2 h at room temperature. Coverslips were mounted on glass slides with ProLong Diamond antifade reagent (Invitrogen, Life Technologies Corporation, Eugene, OR, USA).
Z-stack images of neuronal cells were taken in steps of 1 μm for a total range of 5–6 μm at 200× magnification with a Zeiss LSM710 confocal microscope and analyzed with Imaris software (version 7.6.4 X64, Bitplane, Zurich, Switzerland). Filament tracer module of Imaris package automatically detects cell bodies, tracks neurites in 3D, and quantifies the neurite length in μm. Cell bodies were excluded from our image analyses, and the total neurite length was normalized by the number of cell bodies in each image, thus producing a value of neurite length in μm per neuron. Forty to 60 neurons were analyzed per condition for each mouse, and the average values for one animal were used to calculate the group means.

2.13. Statistical analyses

Categorical variables were compared using the chi-square (χ^2) test and expressed as percentages of participants. Continuous data were assessed using the parametric *t*-test or nonparametric Mann–Whitney U test and expressed as mean ± SD or mean ± SEM. Wilcoxon matched-pairs signed rank test and repeated measures one-way analysis of variance (ANOVA) test were applied to assess the effect of different treatment conditions on SH-SY5Y and primary cells. Linear multivariable least square and logistic regression analyses were performed to determine associations between two variables.
In experimental settings, multiple linear regression analyses were used to model the effect of magnesium and methylglyoxal on outcomes of neuronal cell morphology such as neurite count, length, width, and branch point numbers. To reduce batch (experiment) to batch variability, the observed morphological measures were batch adjusted before analyses (by adding the difference of the overall mean and the batch mean).
All statistical tests were performed two-sided. The level of significance was set at $\alpha = 0.05$. All analyses were performed using SAS v9.4 (Cary, NC, USA) or SPSS v22.0 (Chicago, IL, USA) software. Graphs were generated using GraphPad Prism 6 (La Jolla, CA, USA) software.

3. RESULTS

3.1. Plasma methylglyoxal concentrations are similar in recently diagnosed type 2 diabetes patients with and without DSPN

Here, we studied 235 individuals recently diagnosed with type 2 diabetes from the prospective GDS [31] baseline cohort, 22% (n = 51) of whom had DSPN ($DSPN^+$) and 78% (n = 184) did not have DSPN ($DSPN^-$) (Table 1). Among the 235 individuals from the baseline cohort studied, 54% (n = 127) had a follow-up after 5 years (Table 2).
The mean plasma concentration of methylglyoxal did not differ between $DSPN^+$ and $DSPN^-$ individuals (mean ± SEM: 304 ± 18 nM vs 276 ± 8 nM). Serum magnesium concentrations were reduced in the $DSPN^+$ group compared to that in the $DSPN^-$ group (Figure 1A). In addition, the magnesium concentration was inversely associated with methylglyoxal (Figure 1B) and HbA_{1c} ($\beta = -0.352/p = 0.012$) levels in the $DSPN^+$ group.

3.2. Circulating methylglyoxal, magnesium, and their interaction are strongly associated with DSPN

While plasma methylglyoxal concentration per se was not associated with DSPN, comprehensive statistical analyses revealed a striking association of circulating methylglyoxal concentrations and DSPN when the interaction of circulating magnesium and methylglyoxal was included in the logistic regression model (Figure 1C). In addition, circulating methylglyoxal was associated with lower peroneal motor nerve conduction velocity (Figure 1D), higher warm thermal detection threshold (TDT) (Figure 1E) and lower cold TDT (Figure 1F) on the foot. Of note, increasing magnesium concentrations abolished and reversed the adverse effect of methylglyoxal for all parameters (Figure 1C–F). The interaction of magnesium and methylglyoxal was also predictive for changes in the warm (Figure 1G) and cold (Figure 1H) TDT on the foot over five years. Based on these findings and the fact that magnesium is required for the catalytic activity of enzymes involved in carbohydrate metabolism, we hypothesized that magnesium could be neuroprotective in the context of DSPN by preventing potential methylglyoxal-mediated neuronal injury.

Table 1 — Demographic and clinical characteristics.

Variable	$DSPN^-$	$DSPN^+$
n (% male)	184 (64)	51 (77)
Diabetes duration (years)	0.0 (0.0; 0.0)	0.0 (0.0; 0.0)
Age (years)	53.9 (44.6; 60.4)	53.7 (48.0; 61.6)
BMI (kg/m^2)	30.6 (27.3; 34.9)	30.7 (27.9; 35.2)
Current smoking status (% yes)	15	16
Heart rate (bpm)	69.1 (62.4; 76.0)	70.0 (63.9; 82.5)[1]
Systolic blood pressure (mmHg)	131 (120; 143)	134 (124; 145)
Diastolic blood pressure (mmHg)	74 (68; 80)	75 (72; 81)
Triglycerides (mg/dl)	126 (89; 189)	142 (88; 206)
Cholesterol (mg/dl)	199 (175; 234)	198 (167; 236)
HDL cholesterol (mg/dl)	46 (39; 54)	46 (38; 58)
LDL cholesterol (mg/dl)	126 (104; 152)	120 (92; 151)
Creatinine (mg/dl)	0.84 (0.74; 1.04)	0.89 (0.74; 0.97)
CRP (mg/dl)	0.30 (0.30; 0.50)	0.30 (0.30; 0.50)
HbA_{1c} (%)	6.2 (5.9; 6.9)	6.6 (6.2; 7.3)
HbA_{1c} (mol/mmol)	44.3 (41.0; 51.9)	48.6 (44.3; 56.3)
Magnesium (mmol/l)	0.86 (0.81; 0.91)	0.84 (0.78; 0.90)[1]
Hypomagnesemia [<0.74 mmol/l] (n/%)	9/4.9	6/11.8
NSS (points)	0.00 (0.00; 0.00)	0.00 (0.00; 4.00)[1]
NDS (points)	0.00 (0.00; 2.00)	2.00 (0.00; 4.00)[1]
Peroneal MNCV (m/s)	46.5 (44.0; 49.0)	38.6 (36.0; 41.1)[1]
Median MNCV (m/s)	54.0 (51.1; 56.9)	49.0 (47.0; 51.0)[1]
Ulnar MNCV (m/s)	56.8 (53.0; 60.0)	50.0 (47.0; 53.6)[1]
Sural SNCV (m/s)	46.0 (42.9; 49.0)	38.9 (35.0; 42.0)[1]
Median SNCV (m/s)	52.0 (48.0; 57.0)	49.0 (46.0; 54.4)[1]
Ulnar SNCV (m/s)	54.0 (51.0; 57.1)	52.0 (46.8; 55.0)[1]
Sural SNAP (μV)	8.83 (6.49; 12.23)	3.63 (1.81; 5.41)[1]
Median SNAP (μV)	5.55 (3.77; 7.73)	3.28 (1.81; 5.50)[1]
Ulnar SNAP (μV)	4.92 (2.85; 6.76)	2.60 (1.34; 3.99)[1]
Metacarpal VPT (μm)	0.36 (0.22; 0.60)	0.48 (0.30; 0.72)
Malleolar VPT (μm)	1.08 (0.48; 2.11)	2.05 (0.93; 4.25)
TDT hand cold (C°)	30.3 (29.9; 30.8)	30.4 (29.6; 30.8)
TDT hand warm (C°)	33.9 (33.4; 34.5)	34.2 (33.6; 34.8)
TDT foot cold (C°)	28.9 (26.3; 30.1)	27.7 (25.7; 29.4)[1]
TDT foot warm (C°)	39.2 (36.3; 42.8)	42.7 (38.3; 45.8)[1]

Data are presented as % or median (1st; 3rd quartile). [1]P < 0.05 vs $DSPN^-$ (adjusted for sex, age, BMI, and smoking status).
Abbreviations: BMI, body mass index; CRP, C-reactive protein; DSPN, diabetic sensorimotor polyneuropathy; HbA1c, hemoglobin A1c; HDL, high-density lipoprotein; LDL, low-density lipoprotein; MNCV, motor nerve conduction velocity; NDS, neuropathy disability score; NSS, neuropathy symptom score; SNAP, sensory nerve action potential; SNCV, sensory nerve conduction velocity; TDT, thermal detection thresholds; VPT, vibration perception threshold.

3.3. Magnesium prevents methylglyoxal-mediated neurotoxicity

To determine the neurotoxic effect of methylglyoxal and the putative neuroprotective effect of magnesium *in vitro*, differentiated neuron-like SH-SY5Y cells were exposed to methylglyoxal alone (0, 400, and 800 μM) or in the presence of 30 mM $MgCl_2$ for 24 h. The positive effect of magnesium supplementation on the cell number

Table 2 — Demographic and clinical characteristics of the prospective GDS cohort.

Variable	Baseline	5y follow-up
n (% male)	127 (72)	127 (72)
Diabetes duration (months)	5.0 (3.0; 7.0)	66.0 (63.0; 68.0)
Age (years)	52.9 (45.8; 62.7)	58.3 (50.9; 67.0)
BMI (kg/m^2)	31.0 (27.3; 35.2)	30.4 (27.7; 35.7)
Current smoking status (% yes)	13.4	18.9
Heart rate (bpm)	69.3 (64.7; 77.6)	70.5 (63.5; 77.7)
Systolic blood pressure (mmHg)	131 (122; 144)	132 (122; 144)
Diastolic blood pressure (mmHg)	74 (69; 82)	73 (66; 78)[1]
Triglycerides (mg/dl)	127 (89; 204)	143 (99; 237)[1]
Cholesterol (mg/dl)	199 (169; 231)	203 (175; 235)
HDL cholesterol (mg/dl)	46 (38; 55)	47 (39; 58)
LDL cholesterol (mg/dl)	123 (96; 151)	127 (104; 153)[1]
Creatinine (mg/dl)	0.94 (0.84; 1.04)	0.87 (0.73; 0.98)[1]
CRP (mg/dl)	0.24 (0.13; 0.50)	0.19 (0.09; 0.35)[1]
HbA_{1c} (%)	6.2 (5.9; 6.9)	6.6 (6.2; 7.3)[1]
HbA_{1c} (mol/mmol)	44.3 (41.0; 51.9)	48.6 (44.3; 56.3)[1]
Magnesium (mmol/l)	0.86 (0.81; 0.91)	0.83 (0.80; 0.88)[1]
Hypomagnesemia [<0.74 mmol/l] (n/%)	7/5.5	8/6.3
DSPN (%)	19.7	21.6
NSS (points)	0.00 (0.00; 0.00)	0.00 (0.00; 0.00)
NDS (points)	2.00 (0.00; 3.00)	2.00 (0.00; 4.00)
Peroneal MNCV (m/s)	45.0 (41.0; 48.0)	44.0 (40.0; 46.0)[1]
Median MNCV (m/s)	53.0 (50.9; 56.0)	53.0 (49.0; 55.0)[1]
Ulnar MNCV (m/s)	56.0 (51.8; 59.0)	54.0 (52.0; 57.0)[1]
Sural SNCV (m/s)	45.0 (40.3; 48.3)	44.0 (40.0; 48.0)[1]
Median SNCV (m/s)	52.0 (47.1; 57.7)	51.0 (45.0; 56.0)
Ulnar SNCV (m/s)	54.0 (51.0; 56.6)	52.0 (48.0; 55.0)[1]
Sural SNAP (μV)	8.07 (4.46; 11.41)	7.06 (4.07; 9.22)[1]
Median SNAP (μV)	5.14 (3.30; 7.60)	4.62 (3.00; 6.68)
Ulnar SNAP (μV)	4.08 (2.34; 6.68)	3.89 (2.40; 5.64)
Metacarpal VPT (μm)	0.37 (0.23; 0.56)	0.53 (0.36; 0.93)[1]
Malleolar VPT (μm)	1.11 (0.52; 2.38)	1.96 (0.97; 4.71)[1]
TDT hand cold (C°)	30.4 (29.8; 30.8)	30.6 (30.2; 31.0)[1]
TDT hand warm (C°)	33.9 (33.4; 34.5)	33.8 (33.3; 34.5)
TDT foot cold (C°)	28.2 (25.9; 30.0)	28.1 (26.0; 29.6)
TDT foot warm (C°)	39.9 (36.7; 43.1)	39.9 (37.0; 43.5)

Data are presented as % or median (1st; 3rd quartile). [1]P < 0.05 vs baseline (Wilcoxon matched-pairs signed rank test).
Abbreviations: BMI, body mass index; CRP, C-reactive protein; DSPN, diabetic sensorimotor polyneuropathy; HbA_{1c}, hemoglobin A_{1c}; HDL, high-density lipoprotein; LDL, low-density lipoprotein; MNCV, motor nerve conduction velocity; NDS, neuropathy disability score; NSS, neuropathy symptom score; SNAP, sensory nerve action potential; SNCV, sensory nerve conduction velocity; TDT, thermal detection thresholds; VPT, vibration perception threshold.

and morphology in the presence of methylglyoxal was readily discernible by comparing cell images (Figure 2A). To obtain a comprehensive overview on the impact of the different treatment conditions on the neuronal cell integrity (neurite count, length, width, and branch point numbers), high-content image analyses were performed. We first fitted a full model by estimating separate means for all experimental settings. For all outcomes, the full model can be simplified to a linear dose-response relationship of methylglyoxal without interaction with magnesium treatment (different intercepts, equal slopes for the magnesium treated and untreated experimental groups). R^2 differences with respect to the full model ranged from 0.8% to 5% and the corresponding *P*-values from 0.74 to 0.1. For neurite count and length, the simplified models are illustrated in Figure 2B. In all models, the intercept in the magnesium-treated group was strikingly lower than in the untreated group (all $P \leq 1.6^{-7}$). Moreover, the common slope of the regression lines was different from zero (all $P \leq 10^{-7}$). To compare the protective effect of magnesium between different outcomes of neuronal cell morphology, we estimated the concentration of methylglyoxal at which the neurotoxic effect can be compensated by 30 mM of $MgCl_2$ by calculating the horizontal distance of the two parallel regression lines. For all morphological measures, these levels turned out to be similar with a mean methylglyoxal concentration of 696 μM (range: 610—784 μM). The protective effect was magnesium specific because supplementation with the divalent cations zinc and manganese had no effect on methylglyoxal neurotoxicity (Figure 2C).

3.4. The neuroprotective effect of magnesium results from intracellular reduction of methylglyoxal production

Methylglyoxal-mediated neurotoxicity depends on the detrimental protein/DNA modifications. The analyses of cell lysates for methylglyoxal 5-hydro-5-methylimidazolone (MG-H1) protein modifications showed that magnesium supplementation leads to a reduction of MG-H1 (Figure 2D). Further assessments revealed that magnesium had no effect on supplemented methylglyoxal. The difference in the mean ratio of MG-H1 modifications between medium alone and magnesium supplemented medium was 0.84. After adjustment for the effect of magnesium alone, the MG-H1 modification levels of the corresponding samples without and with magnesium were almost identical (Figure 2E). Therefore, the neuroprotective effect of magnesium resulted exclusively from the reduction of intracellular methylglyoxal formation only.

3.5. Magnesium supplementations prevents neurite degeneration in DRGs resulting from downregulation of mitochondrial activity

Mitochondrial dysfunction has been implicated in the development of DSPN [39]. There are several enzymes involved in glucose metabolism, including mitochondrial function, that require magnesium as cofactor [20—22]. Alterations in mitochondrial activity and resulting impaired glucose metabolism lead to enrichment of triosephosphates, the primary source of methylglyoxal. Therefore, we aimed to determine whether the downregulation of mitochondrial function in mouse DRG cells would have an effect on neurite outgrowth and if so, whether magnesium supplementation can reverse the negative impact. As shown in Figure 2F, the downregulation of mitochondrial activity using a pyruvate dehydrogenase (CPI-613) and mitochondrial complex III (Antimycin A) inhibitor resulted in a 28% reduction of neurite length. Magnesium supplementation completely reversed the adverse effect of CPI-613 and Antimycin A.

4. DISCUSSION

AGEs and their receptor (RAGE) have been implicated in the development of neurodegenerative disorders [40]. However, the impact of glycation processes on the development and progression of diabetic neuropathy in humans remains unclear. Hansen et al. could not find an association between serum methylglyoxal and DSPN in longer-term type 2 diabetes patients [17]. In contrast, other studies showed associations of AGEs and methylglyoxal hydroimidazolone with DSPN in patients with long-term type 1 diabetes [16,18]. The ADDITION-Denmark study identified higher methylglyoxal levels as a risk factor for incident DSPN [41]. Here, we demonstrate that while plasma methylglyoxal concentrations were similar, serum magnesium concentrations were reduced in recently diagnosed type 2 diabetes patients with DSPN compared to those with no DSPN. Serum magnesium concentrations were also inversely associated with plasma methylglyoxal levels in the DSPN group. Surprisingly, magnesium, methylglyoxal,

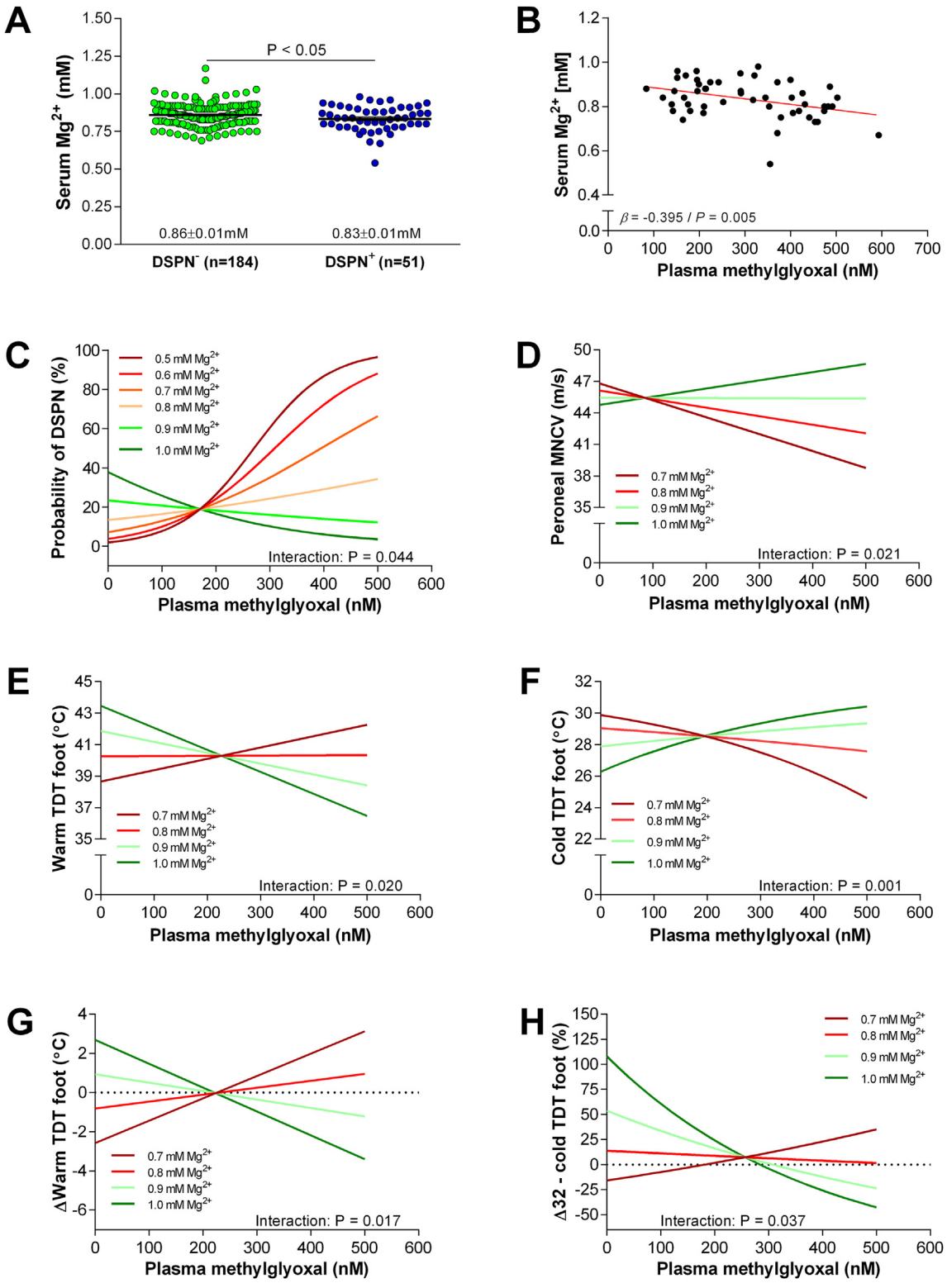

Figure 1: Serum magnesium concentration is inversely associated with methylglyoxal concentration and modulates the association of methylglyoxal with nerve function. (A) Serum magnesium concentration in the $DSPN^{+}$ and $DSPN^{-}$ group. (B) Inverse association of serum magnesium and plasma methylglyoxal in $DSPN^{+}$ patients from the German Diabetes Study (GDS). (C) Predicted association of methylglyoxal and DSPN for selected magnesium concentrations. (D and F) Predicted associations of plasma methylglyoxal with peroneal motor nerve conduction velocity (MNCV), warm thermal detection thresholds (TDT), and cold TDT were at different magnesium concentrations. (G and H) Predicted methylglyoxal associated changes in warm and cold TDT over five years for selected serum magnesium concentrations (Note: To obtain an approximate normal distribution, we transformed the cold threshold in H to $\log_e(\Delta 32 - \text{cold TDT})$ before analyses. To achieve the original scale after calculating the models, the results could only be reported as % of ($\Delta 32$ − cold TDT) and not as absolute values. Therefore, the pattern of the color lines for the cold threshold is reversed in H compared to F). For (A), data are represented as mean ± SEM.

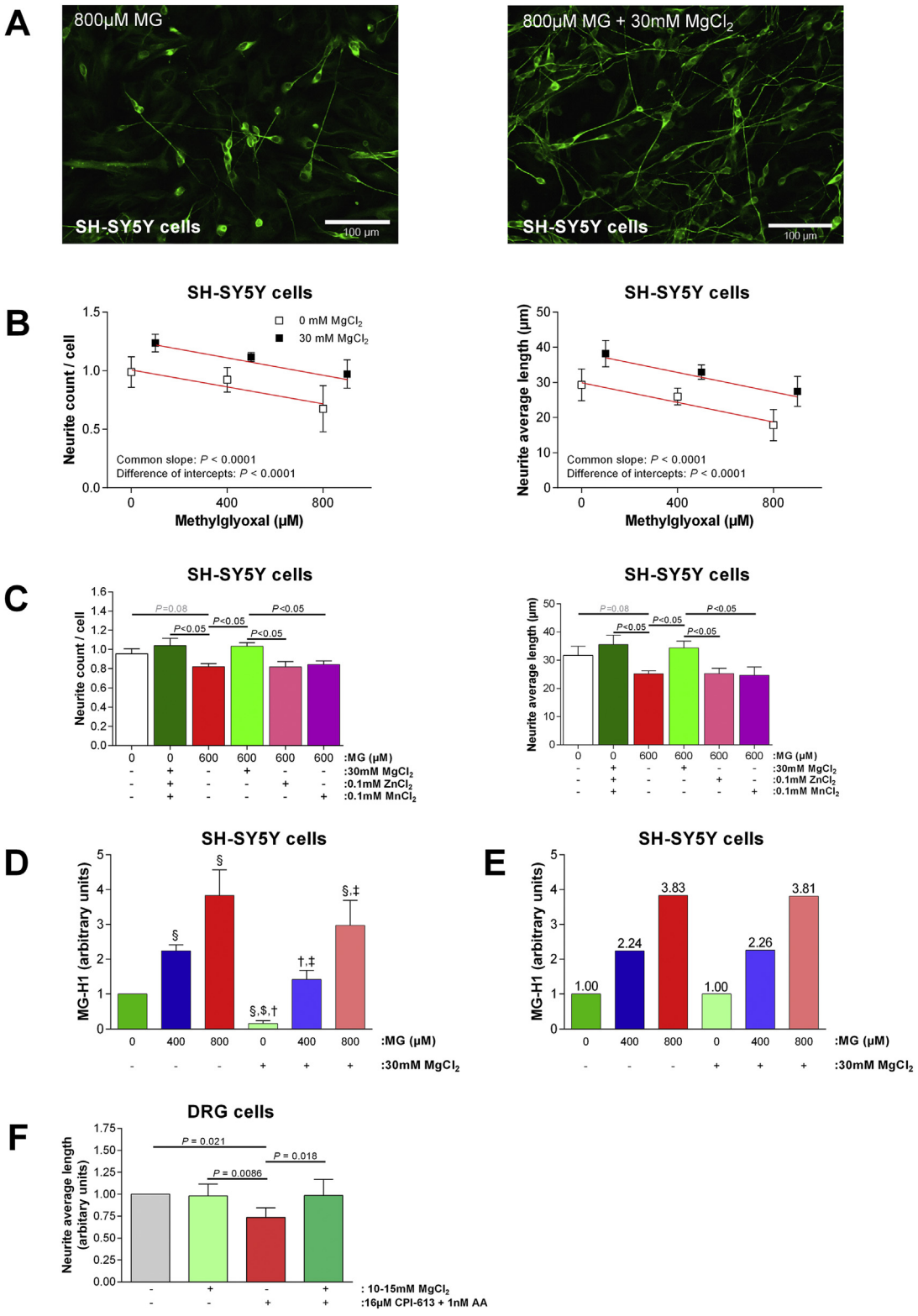

Figure 2: Magnesium supplementation reduces intracellular methylglyoxal formation and attenuates methylglyoxal neurotoxicity. (A) Representative images of methylglyoxal treated SH-SY5Y cells with and without magnesium supplementation. (B) Neuronal cell integrity under different treatment conditions with methylglyoxal and/or magnesium. (C) The effect of different divalent cations alone or in the presents of 600 µM methylglyoxal on neuronal cell integrity. (D) Overall level of methylglyoxal-mediated MG-H1 modifications under different conditions. ($P < 0.05$ vs §control; $^{\$}$400 µM MG; †800 µM MG; ‡30 mM $MgCl_2$) (E) The level of MG-H1 modifications after adjustment for the intracellular methylglyoxal reduction. (F) Effect of pyruvate dehydrogenase inhibitor (CPI-613), complex III inhibitor (Antimycin A [AA]), and magnesium on neurite outgrowth in primary mouse dorsal root ganglia cells. Data combined from (B) 8, (D) 6, and (C and F) 4 independent experiments are displayed as mean ± SD for B and F and mean ± SEM for C and D.

and importantly their interaction were strongly associated with the probability of having DSPN as well as nerve dysfunction. Under experimental conditions, supplementation with magnesium exerted a prominent neuroprotective effect against methylglyoxal-neurotoxicity by reducing MG-H1 protein modifications. Of note, magnesium had no effect on MG-H1 modifications caused by supplemented methylglyoxal. However, it prevented intracellular methylglyoxal formation, which was sufficient to mediate an overall neuroprotective effect in methylglyoxal-treated cells. These observations support our clinical findings and suggest that at higher systemic magnesium concentrations, the adverse associations of higher systemic methylglyoxal levels with DSPN and nerve dysfunction are reversed. Based on these two independent observations, using a translational approach, it may be speculated that in individuals with type 2 diabetes higher magnesium levels lead to lower intracellular methylglyoxal levels. This in turn results in a neuroprotective effect by reducing the intracellular level of the detrimental MG-H1 protein modifications. Inhibition of mitochondrial function and consequently the cellular accumulation of triosephosphates, the primary source of methylglyoxal, resulted in neurite degeneration in primary mouse DRG cells. Magnesium supplementation completely reversed neurite degeneration resulting from inhibition of mitochondrial activity in DRG cells.

Based on the published data and our findings discussed above, we propose a novel link between hypomagnesemia, carbonyl stress, and neuronal damage. As shown in Figure 3, magnesium is required for the catalytic activity of the key enzyme of the pentose phosphate pathway and mitochondrial activity [20—22]. Therefore, magnesium deficiency and hyperglycemia result in glyceraldehyde-3-phosphate and subsequently dihydroxyacetone phosphate accumulation. This leads to an increased formation of methylglyoxal by methylglyoxal synthase, which is an irreversible reaction. The glyoxalase system is responsible for detoxification of methylglyoxal [3]. Magnesium is one of the major divalent metal ions crucial for the catalytic activity of glyoxalase 1 [42], the rate-limiting step in the methylglyoxal degradation. Therefore, hypomagnesemia leads to methylglyoxal accumulation, formation of detrimental methylglyoxal-mediated protein/DNA modifications, and neurotoxicity.

Magnesium deficiency has been linked to both disturbances in carbohydrate metabolism and type 2 diabetes [23]. Furthermore, type 2 diabetes is associated with impaired mitochondrial function [43,44]. As shown in Figure 3, several enzymes involved in glucose metabolism, including PDH, require magnesium as cofactor for catalytic activity. Under hyperglycemic conditions, the higher glucose flux and impaired mitochondrial function due to magnesium deficiency leads to accumulation of triosephosphates, which in turn leads to increased formation of methylglyoxal [5,8]. Here, we demonstrate that inhibition of mitochondrial activity was associated with neurite degeneration in primary mouse DRGs. This adverse impact of lower mitochondrial activity was completely abolished when the DRG culture was supplemented with 10—15 mM of magnesium. This effect was probably mediated by upregulation of the pentose phosphate pathway (PPP) and mitochondrial activity, thereby reducing the triosephosphate concentration and consequently methylglyoxal formation.

The strengths of the present study are the relatively large sample size of type 2 diabetes patients, the detailed neurophysiological

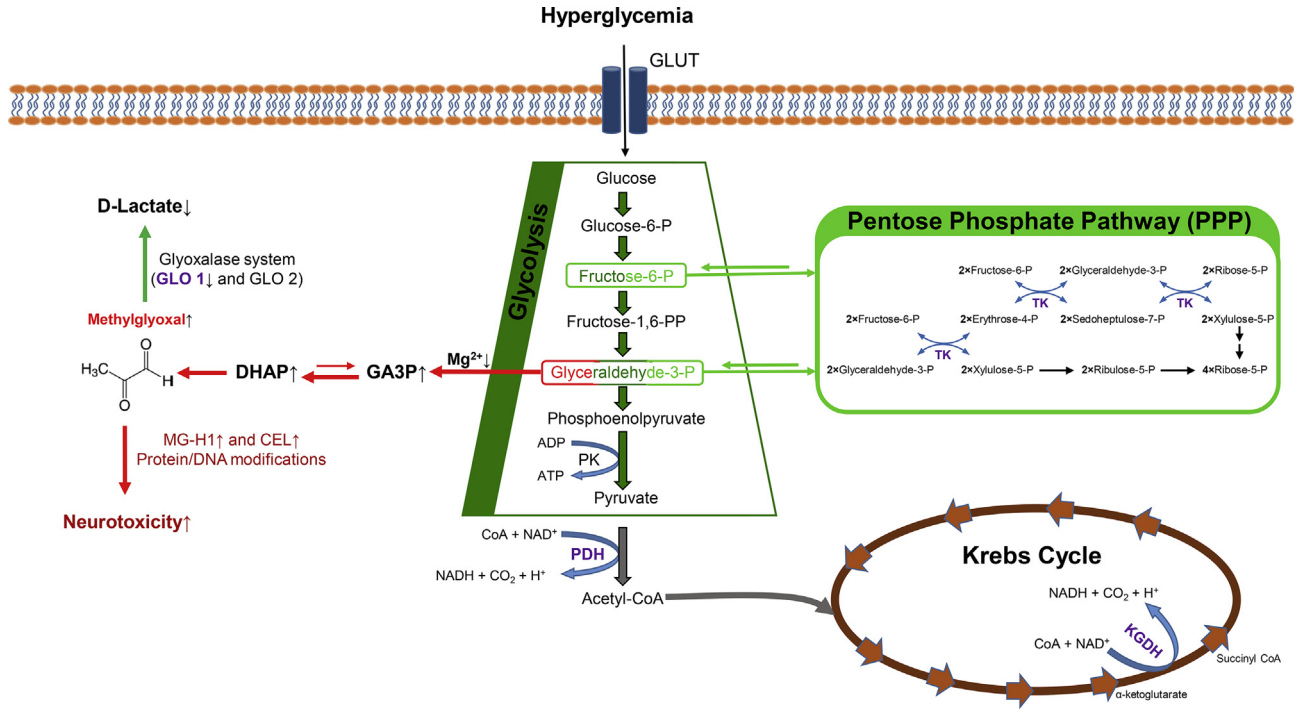

Figure 3: Schematic mechanism of hypomagnesemia-mediated overproduction of methylglyoxal leading to neurotoxicity. Hyperglycemia results in an increased glucose influx, which is metabolized in mitochondria (Krebs cycle) or alternatively through the PPP. Several enzymes involved in glucose metabolism require magnesium for catabolic activity (marked purple). Hypomagnesemia ($Mg^{2+}\downarrow$) leads to reduced glucose metabolism in mitochondria and pentose phosphate pathway (PPP), increased levels of glyceraldehyde-3-phosphate (GA3P), and consequently dihydroxyacetone phosphate (DHAP). This results in increased formation of methylglyoxal from DHAP by methylglyoxal synthase (irreversible reaction). The accumulation of methylglyoxal leads to an increased level of detrimental methylglyoxal-mediated protein/DNA modifications and neurotoxicity. Abbreviations: CEL, N(epsilon)-(1-carboxyethyl)lysine; GLO1, glyoxalase 1; GLO2, glyoxalase 2; GLUT, glucose transporter; KGDH, α-ketoglutarate dehydrogenase; MG-H1, methylglyoxal 5-hydro-5-methylimidazolone; PDH, pyruvate dehydrogenase; PK, pyruvate kinase; TK, transketolase.

assessment using sophisticated methodology, comprehensive statistical analyses, and the detailed characterization of the neuronal cell morphology using high-content image analysis. Moreover, multiple data acquiring approaches were used that provided supportive results for the hypothesis. These included a translational approach ranging from human sampling to primary animal cells to cell culture. There are also some caveats to consider. First, our findings apply only to individuals with recent onset rather than long-term diabetes. Second, although a control group with normal glucose tolerance and magnesium measurements is part of the GDS, methylglyoxal concentrations data for comparison with the type 2 diabetes groups were not available. Third, the association of magnesium, methylglyoxal, and their interaction with nerve dysfunction is based on single snapshot values. Data from multiple measurements over time for magnesium and methylglyoxal would be more robust. Fourth, the impact of magnesium on mitochondrial activity and MG-H1 protein modifications were not determined in DRGs. Fifth, the neuroprotective effect of magnesium was assessed using human neuroblastoma cells and mouse peripheral neuronal cells. Future studies are needed to further characterize the neuroprotective effect of magnesium using human peripheral neuronal cells and under clinical settings.

In conclusion, because hypomagnesemia is associated with both DSPN and increased methylglyoxal levels, magnesium supplementation could be a promising therapy to protect from carbonyl stress-induced nerve damage in DSPN.

AUTHORS' CONTRIBUTIONS

A.S. and D.Z. designed the experiments and wrote the article. A.S., E.D., F.Z., H.S., M.S., R.R., T.H.F., and B.F.B performed the experiments. G.B., K.M., J.S., M.R., and D.Z. conducted clinical observations. A.S., K.S., B.F.B, R.R., M.S., B.B., M.Y., and D.Z. analyzed the data. B.B., B.F.B, E.D., G.B., H.S., J.S., M.S., M.Y., R.R., K.M., K.S., E.F., P.P.N., T.H.F., V.B., and M.R. contributed to the discussion and reviewed and edited the article. D.Z. is the guarantor of this work and, as such, had full access to all the data in the study and takes responsibility for the integrity of the data and the accuracy of the data analysis. All authors had access to all the data and approved the final version of the manuscript.

ACKNOWLEDGMENTS

The authors wish to thank the staff of the GDS, especially M. Schroers-Teuber, J. Schubert, F. Battiato, J. Busch, N. Krahnke-Schoelzel, and B. Ringel for their excellent technical support. The authors also wish to thank Prof. H. Finner for helpful discussions regarding statistical analysis and Prof. F.W. Scott for critically reading the manuscript. The experimental studies were supported by the German Center for Diabetes Research (DZD) Grant Number FKZ82DZD00202 and in part by German Diabetes Association award (A.S.), German Diabetes Center Training and Feasibility Grant (A.S), and National Institute of Diabetes and Digestive and Kidney Diseases of the National Institutes of Health award [DK107339-04] (M.Y.). The GDS study was supported by the Ministry of Culture and Science of the State of North Rhine-Westphalia (MKW NRW), the German Federal Ministry of Health (BMG), and in part by a grant of the Federal Ministry for Research (BMBF) to the German Center for Diabetes Research. For the GDS group: M. Roden, H. Al-Hasani, A. E. Buyken, B. Belgardt, G. Geerling, C. Herder, A. Icks, J. Kotzka, O. Kuß, E. Lammert,J-H. Hwang, K. Müssig, D. Markgraf, W. Rathmann, J. Szendroedi & D. Ziegler.

CONFLICTS OF INTEREST

None declared.

REFERENCES

[1] Pop-Busui, R., Boulton, A.J., Feldman, E.L., Bril, V., Freeman, R., Malik, R.A., et al., 2017. Diabetic neuropathy: a position statement by the American diabetes association. Diabetes Care 40(1):136–154.

[2] Kalapos, M.P., 2013. Where does plasma methylglyoxal originate from? Diabetes Research and Clinical Practice 99(3):260–271.

[3] Sousa Silva, M., Gomes, Ricardo A., Ferreira, Antonio E.N., Ponces Freire, A., Cordeiro, C., 2013. The glyoxalase pathway: the first hundred years… and beyond. Biochemical Journal 453(1):1–15.

[4] Fleming, T., Cuny, J., Nawroth, G., Djuric, Z., Humpert, P.M., Zeier, M., et al., 2012. Is diabetes an acquired disorder of reactive glucose metabolites and their intermediates? Diabetologia 55(4):1151–1155.

[5] McLellan, A.C., Phillips, S.A., Thornalley, P.J., 1992. The assay of methylglyoxal in biological systems by derivatization with 1,2-diamino-4,5-dimethoxybenzene. Analytical Biochemistry 206(1):17–23.

[6] Moraru, A., Wiederstein, J., Pfaff, D., Fleming, T., Miller, A.K., Nawroth, P., et al., 2018. Elevated levels of the reactive metabolite methylglyoxal recapitulate progression of type 2 diabetes. Cell Metabolism 27(4):926–934 e928.

[7] Tilton, R.G., Baier, L.D., Harlow, J.E., Smith, S.R., Ostrow, E., Williamson, J.R., 1992. Diabetes-induced glomerular dysfunction: links to a more reduced cytosolic ratio of NADH/NAD+. Kidney International 41(4):778–788.

[8] Thornalley, P.J., Jahan, I., Ng, R., 2001. Suppression of the accumulation of triosephosphates and increased formation of methylglyoxal in human red blood cells during hyperglycaemia by thiamine in vitro. Journal of Biochemistry 129(4):543–549.

[9] Bierhaus, A., Fleming, T., Stoyanov, S., Leffler, A., Babes, A., Neacsu, C., et al., 2012. Methylglyoxal modification of Nav1.8 facilitates nociceptive neuron firing and causes hyperalgesia in diabetic neuropathy. Nature Medicine 18(6):926–933.

[10] Cullum, N.A., Mahon, J., Stringer, K., McLean, W.G., 1991. Glycation of rat sciatic nerve tubulin in experimental diabetes mellitus. Diabetologia 34(6):387–389.

[11] Ryle, C., Donaghy, M., 1995. Non-enzymatic glycation of peripheral nerve proteins in human diabetics. Journal of Neurological Sciences 129(1):62–68.

[12] Vlassara, H., Brownlee, M., Cerami, A., 1981. Nonenzymatic glycosylation of peripheral nerve protein in diabetes mellitus. Proceedings of the National Academy of Sciences of the United States of America 78(8):5190–5192.

[13] Cameron, N.E., Gibson, T.M., Nangle, M.R., Cotter, M.A., 2005. Inhibitors of advanced glycation end product formation and neurovascular dysfunction in experimental diabetes. Annals of the New York Academy of Sciences 1043:784–792.

[14] Juranek, J.K., Geddis, M.S., Song, F., Zhang, J., Garcia, J., Rosario, R., et al., 2013. RAGE deficiency improves postinjury sciatic nerve regeneration in type 1 diabetic mice. Diabetes 62(3):931–943.

[15] Wada, R., Nishizawa, Y., Yagihashi, N., Takeuchi, M., Ishikawa, Y., Yasumura, K., et al., 2001. Effects of OPB-9195, anti-glycation agent, on experimental diabetic neuropathy. European Journal of Clinical Investigation 31(6):513–520.

[16] Genuth, S., Sun, W., Cleary, P., Gao, X., Sell, D.R., Lachin, J., et al., 2015. Skin advanced glycation end products glucosepane and methylglyoxal hydroimidazolone are independently associated with long-term microvascular complication progression of type 1 diabetes. Diabetes 64(1):266–278.

[17] Hansen, C.S., Jensen, T.M., Jensen, J.S., Nawroth, P., Fleming, T., Witte, D.R., et al., 2015. The role of serum methylglyoxal on diabetic peripheral and cardiovascular autonomic neuropathy: the ADDITION Denmark study. Diabetic Medicine 32(6):778–785.

[18] Sveen, K.A., Karime, B., Jorum, E., Mellgren, S.I., Fagerland, M.W., Monnier, V.M., et al., 2013. Small- and large-fiber neuropathy after 40 years of type 1 diabetes: associations with glycemic control and advanced protein glycation: the Oslo Study. Diabetes Care 36(11):3712–3717.

[19] de Baaij, J.H., Hoenderop, J.G., Bindels, R.J., 2015. Magnesium in man: implications for health and disease. Physiological Reviews 95(1):1—46.
[20] Wieland, O.H., 1983. The mammalian pyruvate dehydrogenase complex: structure and regulation. Reviews of Physiology, Biochemistry & Pharmacology 96:123—170.
[21] Panov, A., Scarpa, A., 1996. Independent modulation of the activity of alpha-ketoglutarate dehydrogenase complex by Ca2+ and Mg2+. Biochemistry 35(2):427—432.
[22] Eisinger, J., Bagneres, D., Arroyo, P., Plantamura, A., Ayavou, T., 1994. Effects of magnesium, high energy phosphates, piracetam and thiamin on erythrocyte transketolase. Magnesium Research 7(1):59—61.
[23] Mooren, F.C., 2015. Magnesium and disturbances in carbohydrate metabolism. Diabetes, Obesity and Metabolism 17(9):813—823.
[24] Gommers, L.M., Hoenderop, J.G., Bindels, R.J., de Baaij, J.H., 2016. Hypomagnesemia in type 2 diabetes: a vicious circle? Diabetes 65(1):3—13.
[25] Zhang, Q., Ji, L., Zheng, H., Li, Q., Xiong, Q., Sun, W., et al., 2018. Low serum phosphate and magnesium levels are associated with peripheral neuropathy in patients with type 2 diabetes mellitus. Diabetes Research and Clinical Practice 146:1—7.
[26] Chu, C., Zhao, W., Zhang, Y., Li, L., Lu, J., Jiang, L., et al., 2016. Low serum magnesium levels are associated with impaired peripheral nerve function in type 2 diabetic patients. Scientific Reports 6:32623.
[27] Hasanein, P., Parviz, M., Keshavarz, M., Javanmardi, K., Mansoori, M., Soltani, N., 2006. Oral magnesium administration prevents thermal hyperalgesia induced by diabetes in rats. Diabetes Research and Clinical Practice 73(1):17—22.
[28] Pan, H.C., Sheu, M.L., Su, H.L., Chen, Y.J., Chen, C.J., Yang, D.Y., et al., 2011. Magnesium supplement promotes sciatic nerve regeneration and down-regulates inflammatory response. Magnesium Research 24(2):54—70.
[29] Pearce, A., Lockwood, C., van den Heuvel, C., Pearce, J., 2017. The use of therapeutic magnesium for neuroprotection during global cerebral ischemia associated with cardiac arrest and cardiac surgery in adults: a systematic review. JBI Database of Systematic Reviews and Implementation Reports 15(1):86—118.
[30] Zhao, B., Deng, H., Li, B., Chen, L., Zou, F., Hu, L., et al., 2019. Association of magnesium consumption with type 2 diabetes and glucose metabolism: a systematic review and pooled study with trial sequential analysis. Diabetes Metabolism Research and Reviews e3243.
[31] Szendroedi, J., Saxena, A., Weber, K.S., Strassburger, K., Herder, C., Burkart, V., et al., 2016. Cohort profile: the German diabetes study (GDS). Cardiovascular Diabetology 15:59.
[32] Ziegler, D., Papanas, N., Zhivov, A., Allgeier, S., Winter, K., Ziegler, I., et al., 2014. Early detection of nerve fiber loss by corneal confocal microscopy and skin biopsy in recently diagnosed type 2 diabetes. Diabetes 63(7):2454—2463.
[33] Young, M.J., Boulton, A.J., MacLeod, A.F., Williams, D.R., Sonksen, P.H., 1993. A multicentre study of the prevalence of diabetic peripheral neuropathy in the United Kingdom hospital clinic population. Diabetologia 36(2):150—154.
[34] Dyck, P.J., Albers, J.W., Andersen, H., Arezzo, J.C., Biessels, G.J., Bril, V., et al., 2011. Diabetic polyneuropathies: update on research definition, diagnostic criteria and estimation of severity. Diabetes Metabolism Research and Reviews 27(7):620—628.
[35] Rabbani, N., Thornalley, P.J., 2014. Measurement of methylglyoxal by stable isotopic dilution analysis LC-MS/MS with corroborative prediction in physiological samples. Nature Protocols 9(8):1969—1979.
[36] de Oliveira, M.R., Ferreira, G.C., Schuck, P.F., Dal Bosco, S.M., 2015. Role for the PI3K/Akt/Nrf2 signaling pathway in the protective effects of carnosic acid against methylglyoxal-induced neurotoxicity in SH-SY5Y neuroblastoma cells. Chemico-Biological Interactions 242(Supplement C):396—406.
[37] Malin, S.A., Davis, B.M., Molliver, D.C., 2007. Production of dissociated sensory neuron cultures and considerations for their use in studying neuronal function and plasticity. Nature Protocols 2(1):152—160.
[38] Singh, B., Xu, Y., McLaughlin, T., Singh, V., Martinez, J.A., Krishnan, A., et al., 2012. Resistance to trophic neurite outgrowth of sensory neurons exposed to insulin. Journal of Neurochemistry 121(2):263—276.
[39] Chandrasekaran, K., Anjaneyulu, M., Choi, J., Kumar, P., Salimian, M., Ho, C.Y., et al., 2019. Role of mitochondria in diabetic peripheral neuropathy: influencing the NAD(+)-dependent SIRT1-PGC-1alpha-TFAM pathway. International Review of Neurobiology 145:177—209.
[40] Juranek, J., Ray, R., Banach, M., Rai, V., 2015. Receptor for advanced glycation end-products in neurodegenerative diseases. Reviews in the Neurosciences 26(6):691—698.
[41] Andersen, S.T., Witte, D.R., Dalsgaard, E.-M., Andersen, H., Nawroth, P., Fleming, T., et al., 2018. Risk factors for incident diabetic polyneuropathy in a cohort with screen-detected type 2 diabetes followed for 13 Years: ADDITION-Denmark. Diabetes Care 41(5):1068—1075.
[42] Davis, K.A., Williams, G.R., 1966. Cation activation of glyoxalase I. Biochimica et Biophysica Acta 113(2):393—395.
[43] Patti, M.E., Corvera, S., 2010. The role of mitochondria in the pathogenesis of type 2 diabetes. Endocrine Reviews 31(3):364—395.
[44] Rovira-Llopis, S., Banuls, C., Diaz-Morales, N., Hernandez-Mijares, A., Rocha, M., Victor, V.M., 2017. Mitochondrial dynamics in type 2 diabetes: pathophysiological implications. Redox Biology 11:637—645.

